Title

Single-cell cloning of human T-cell lines reveals clonal variation in cell death responses to chemotherapeutics

Authors

Hanlon, Kathleen
Thompson, Alex
Pantano, Lorena
et al.

Publication Date

2019-09-01

DOI

10.1016/j.cancergen.2019.06.003

Peer reviewed

HHS Public Access

Author manuscript

Cancer Genet. Author manuscript; available in PMC 2020 September 01.

Published in final edited form as:

Cancer Genet. 2019 September ; 237: 69–77. doi:10.1016/j.cancergen.2019.06.003.

Single-cell cloning of human T-cell lines reveals clonal variation in cell death responses to chemotherapeutics

Kathleen Hanlon[a,#], **Alex Thompson**[a,#], **Lorena Pantano**[b], **John N. Hutchinson**[b], **Arshed Al-Obeidi**[a], **Shu Wang**[a], **Meghan Bliss-Moreau**[a], **Jennifer Helble**[c], **Gabriela Alexe**[d], **Kimberly Stegmaier**[d], **Daniel E. Bauer**[a,e], **Ben A. Croker**[a,e,*]

[a]Division of Hematology/Oncology, Boston Children's Hospital, Boston, MA, United States

[b]Department of Biostatistics, Harvard Chan School of Public Health, Boston, MA, United States

[c]Department of Microbiology and Immunobiology, Harvard Medical School, Boston, MA, United States

[d]Department of Pediatric Oncology, Dana-Farber Cancer Institute and Boston Children's Hospital, Boston, MA, United States

[e]Department of Pediatrics, Harvard Medical School, Boston, MA, United States

Abstract

Genetic modification of human leukemic cell lines using CRISPR-Cas9 has become a staple of gene-function studies. Single-cell cloning of modified cells is frequently used to facilitate studies of gene function. Inherent in this approach is an assumption that the genetic drift, amplified in some cell lines by mutations in DNA replication and repair machinery, as well as non-genetic factors will not introduce significant levels of experimental cellular heterogeneity in clones derived from parental populations. In this study, we characterize the variation in cell death of fifty clonal cell lines generated from human Jurkat and MOLT-4 T-cells edited by CRISPR-Cas9. We demonstrate a wide distribution of sensitivity to chemotherapeutics between non-edited clonal human leukemia T-cell lines, and also following CRISPR-Cas9 editing at the *NLRP1* locus, or following transfection with non-targeting sgRNA controls. The cell death sensitivity profile of clonal cell lines was consistent across experiments and failed to revert to the non-clonal parental phenotype. Whole genome sequencing of two clonal cell lines edited by CRISPR-Cas9 revealed unique and shared genetic variants, which had minimal read support in the non-clonal parental population and were not suspected CRISPR-Cas9 off-target effects. These variants included genes related to cell death and drug metabolism. The variation in cell death phenotype of clonal populations of human T-cell lines may be a consequence of T-cell line genetic instability, and to a lesser extent clonal heterogeneity in the parental population or CRISPR-Cas9 off-target effects not predicted by current models. This work highlights the importance of genetic variation between

*Correspondence: Ben A. Croker, Division of Hematology/Oncology, Boston Children's Hospital, Harvard Medical School, 300 Longwood Avenue, Boston, MA 02115 USA. ben.croker@childrens.harvard.edu, Ph: +1-617-919-6288.
#These authors contributed equally to this work.

clonal T-cell lines in the design, conduct, and analysis of experiments to investigate gene function after single-cell cloning.

Keywords

Cell death; leukemia; cloning; T-ALL; chemotherapeutic resistance

INTRODUCTION

CRISPR-Cas9 is a highly versatile approach for genetic manipulation of primary cells and transformed cell lines [1, 2]. However, the gene editing efficiency in some cell types, including human T-cell lines, is highly variable [3, 4]. The human Jurkat T-cell line has been reported to reach editing efficiencies of up to 75% for single edits but lower than 1% for double edits targeting a large kbp region [5, 6]. In the latter case, clonal isolation of cell lines is often used to enable the study of gene function [7, 8]. However, the selection and expansion of a single cell from a genetically diverse population of cells may not accurately represent the parental population [9]. For instance, the isolation of cells bearing mutations that reduce rates of proliferation or increase the sensitivity to cell death generates clonal cell lines for study that may not be expected to survive Darwinian selection pressures of the parental cell population [9]. This is of particular importance when studying responses to cytotoxic chemotherapeutics in clonal lines as the phenotypic response may not be characteristic of the population at whole, as well as when performing genome-wide screening studies where redundancy in genetic editing at each target loci is needed to avoid spurious phenotypic readouts.

While reversion of single-cell clones to a parental phenotype is observed in some cell types for specific phenotypic readouts [10], clonal selection of mutant clones in medulloblastoma following depletion of dominant clones can underlie tumor relapse [11]. Clonal dynamics can be captured in vivo using breast cancer patient-derived xenografts in mice to show evolutionary dominance of specific clones based on genomic aberrations [12]. Genetic instability also profoundly influences the therapeutic responses of patient-derived xenografts in mouse models [13]. In this study, we have investigated whether single-cell cloning may confound the analysis of cell death responses to chemotherapeutics in human T-cell lines. We generated over fifty clonal cell lines by the expansion of single cells from unedited parental, *NLRP-1* targeted CRISPR-Cas9 edited, and non-targeted CRISPR-Cas9 edited Jurkat and MOLT-4 T-cell lines. Clonal cell lines demonstrated wide variability in sensitivity to chemotherapeutics regardless of origin, and a stable cell death phenotype that failed to revert to the phenotype of the parental cell population. Whole genome sequencing demonstrated genetic aberrations found in clonal lines but not the non-clonal parental line that might underlie the wide variation in response to cytotoxic chemotherapeutics. We conclude that functional variation between clonal cell T-cell lines is a factor that must be considered in experimental design and analysis during gene function studies.

MATERIALS AND METHODS

Cell culture

Jurkat and MOLT-4 T-cell lines were cultured in RPMI 1640 (Gibco; 11875–119) and supplemented with 10% Fetal Bovine Serum (Sigma; 12303C), and 100U/ml Penicillin-Streptomycin (Life Technologies; 15140–122). Cells were incubated at 37°C and 5% CO_2. Jurkat cells were maintained in culture at a density of 1×10^5 - 1×10^6 cells/mL. MOLT-4 cells were maintained in culture at a density of 4×10^5 - 2×10^6 cells/mL.

Gene editing of cell lines with Cas9-expressing plasmid

MOLT-4 cells used for whole genome sequencing were edited using a Cas9-expressing plasmid and sgRNAs targeting intron 3 of *NLRP1* (5′-TGT TCT TGC CAT GCG GCG GA-3′) and intron 4 of *NLRP1* (5′-CTC AGG TCA CTC GGG CTT A-3′). The AMAXA cell line nucleofector Kit V (Lonza, NC9041615) was used for transfection as per the manufacturers protocol. A GFP-expressing plasmid was used to monitor transfection efficiency. Transfected cells were sorted for GFP expression by flow cytometry on day 2 or day 3 and single GFP+ cells were plated into 96 well plates. Clones were genotyped by PCR after 2 weeks in culture. Genotyping primers for *NLRP1* include: *NLRP1* intron 4-F: 5′-GAC AGA GCA TGG TGG TCA GA-3′; *NLRP1* exon 4-F: 5′-GCA GCT GTG TGA ATT TTT GG-3′; *NLRP1* exon 4-R: 5′-CGT TTT GTT CCG AGT CTC GT-3′; and *NLRP1* intron 3-R: 5′-TGT GCC AGG TGC TGC TAT AG-3′.

Gene editing of cell lines with RNP complexes

Gene editing of cells used in the viability assays was performed by electroporation of Jurkat and MOLT-4 cells with Alt-R® S.p. Cas9 Nuclease 3NLS (IDT; 1074181) complexed with the Alt-R® CRISPR-Cas9 tracrRNA ATTO 550 (IDT; 1077024) and two crRNAs (IDT) targeting *NLRP1* exon 1 and exon 2, or, as a control, the Alt-R CRISPR-Cas9 Negative Control crRNA #1 (IDT; 1072554) which contains a 20 nt protospacer sequence that is computationally designed to be non-targeting in human reference genomes. The Neon™ Transfection System 10 μL Kit (Thermofisher; MPK1096) was used for transfection as per the manufacturers protocol. After 24 hours, transfected cells were sorted by the presence of the fluorescent tag, ATTO550, attached to the tracrRNA, using flow cytometry. Single ATTO550+ cells were plated into 96 well plates. Genotyping was performed using JumpStart™ REDTaq® ReadyMix™ Reaction Mix (Sigma; P0982) for PCR. Sanger sequencing of gene editing was performed on each clone at the Dana-Farber/ Harvard Cancer Center sequencing core.

crRNA sequences include:

*NLRP1*_Exon 1_target 1: /AltR1/rGrUrA rCrCrU rGrGrU rGrGrC rUrCrA rGrUrA rUrGrG rUrUrU rUrArG rArGrC rUrArU rGrCrU /AltR2/

*NLRP1*_Exon 1_ target 2: /AltR1/rGrCrU rCrCrU rGrGrA rGrUrG rCrGrC rUrUrU rArUrG rUrUrU rUrArG rArGrC rUrArU rGrCrU /AltR2/

*NLRP1*_Exon 1_ target 3: /AltR1/rUrGrG rCrUrC rArGrU rArUrG rGrGrG rArGrC rArGrG rUrUrU rUrArG rArGrC rUrArU rGrCrU /AltR2/

*NLRP1*_Exon 2_ target 1: /AltR1/rGrArU rCrCrA rGrGrG rCrArU rUrArG rCrArC rUrGrG rUrUrU rUrArG rArGrC rUrArU rGrCrU /AltR2/

*NLRP1*_Exon 2_ target 2: /AltR1/rGrGrA rUrCrC rArUrG rArArU rUrGrC rCrGrG rCrGrG rUrUrU rUrArG rArGrC rUrArU rGrCrU /AltR2/

*NLRP1*_Exon 2_ target 3: /AltR1/rGrCrC rCrArA rGrUrG rArArC rCrCrC rArCrC rUrGrG rUrUrU rUrArG rArGrC rUrArU rGrCrU /AltR2/

Genotyping Primers:

NLRP1 Forward- 5′-AGGACAGCACTGTTCTCTGC-3′

NLRP1 Reverse- 5′-GGAACTTCTGGACCACCCTG-3′

Viability assay

Cells were stimulated for 48 hours with either tunicamycin (1μg/mL), doxorubicin (200nM), or paclitaxel (500nM). Viability was assayed using flow cytometry with propidium iodide to discriminate live (PI negative) and dead (PI positive) cells.

Whole genome sequencing

All samples were processed using a genomic variant pipeline implemented in the bcbio-nextgen project (https://bcbio-nextgen.readthedocs.org/en/latest/). Reads were examined for quality issues using FastQC (http://www.bioinformatics.babraham.ac.uk/projects/fastqc/) to ensure library generation and sequencing are suitable for further analysis. Reads were aligned to Ensembl build GChR37 of the Human genome using bwa aligner tool. Structural variant calling was done with Manta 1.0.3 (doi:10.1093/bioinformatics/btv710) generating a VCF file (10.1093/bioinformatics/btr330) with deletion, duplication and translocation events. We annotated variant calls using SnpEff (10.4161/fly.19695) to predict variant effects. Structural variants that appeared in the parental cell line ATCC MOLT-4 were removed from the previous VCF file. Structural variants were analyzed with R 3.5.1 (https://www.r-project.org/) to annotate the gene region affected by each variant with the Bioconductor 3.7 package, annotated (10.1038/nmeth.3252, https://doi.org/10.1093/bioinformatics/btx183). Finally, the data was summarized by gene to quantify the number of unique and shared genes between samples.

Cas-OFFinder [14] was used to search for potential off-target sites for Cas9 RNA-guided endonucleases. We specified the PAM type as SpCas9 from *Streptococcus pyogenes*: 5′-NGG-3′. The target genome for the search was *Homo sapiens* hg19 (GChR37). We set the mismatch number to be less than or equal to 5, the DNA bulge to be less than or equal to 2, and the RNA bulge to be less than or equal to 2, based on possible off-target editing at sites that differ by 5 nt from on-target sites in human cells[15]. We performed separate queries for each of the gRNAs: 5′-TGT TCT TGC CAT GCG GCG GA-3′ and 5′-CTC AGG TCA CTC GGG CTT A-3′. Lastly, we matched each of the variants found by whole genome

sequencing to the closest potential off-target site. If these were closer than 100bp away from each other, we considered them to be potentially off-target variants.

12 structural variants – CDK6, CYP2A6, FGF12, HINT1, HTR2C, MIR137, MYB, POLE2, PTMAP8, RANGAP1, RPS7P4, TPM3P9 – were recalled in the parental ATCC MOLT-4 line and read alignments were visualized using Svviz2 [16].

RESULTS

Variability of cell death between single-cell clones in response to chemotherapeutics

To examine the responses of clonal T-cell lines to cytotoxic chemotherapeutics following CRISPR-Cas9 gene editing, we transfected Jurkat T-cells with sgRNA-Cas9 ribonucleoproteins (RNPs) targeting the cell death gene *NLRP1* and with non-targeting RNPs. We then generated clonal cell lines by the expansion of single cells selected from the non-targeted sgRNA-Cas9 RNP edited (scrambled) population and the *NLRP1*-targeted sgRNA-Cas9 RNP edited population. We confirmed successful editing of *NLRP1* in the clonal lines by PCR. Additionally, to investigate effects of the single cell cloning process, we created clonal lines from Jurkat T-cells which did not undergo electroporation with the CRISPR-Cas9 RNP complex (annotated as parental clones).

To study cell death responses of clonal cell lines, we treated 12 non-edited, 10 scrambled, and 17 *NLRP1*-edited clonal Jurkat T-cell lines with the cytotoxic chemotherapeutic agents doxorubicin and paclitaxel to induce DNA damage or replicative stress, respectively. In untreated samples, all clones maintained similar levels of viability as measured through propidium iodide (PI) staining (Fig. 1a, b). After treatment with doxorubicin or paclitaxel for 48 hours, a wide range in viability was evident in the parental and scrambled control clonal cell lines, equivalent to the 10–95% viability range noted for *NLRP1*-edited clones after paclitaxel treatment (Fig. 1a, b). The pooled median viability of the parental, scrambled, and *NLRP1*-edited clones were 32.98%, 36.35%, and 39.83% after doxorubicin treatment and 27.97%, 27.18% and 38.77% after paclitaxel treatment, respectively (Fig 1a, b). This compares to the average viability of the parental Jurkat population after doxorubicin (50.9±1%) or paclitaxel (59.3±2.9%) treatment (Fig. 1c).

The heterogeneous response of human Jurkat T-cell clones to chemotherapeutics was also observed in a second human T-cell line: MOLT-4 cells. We created 13 non-edited parental, 5 non-targeted CRISPR-Cas9 edited, and 4 *NLRP1*-targeted CRISPR-Cas9 edited clones in MOLT-4 T-cells using the same method as described for Jurkat T-cells. Single-cell clones maintained similar levels of cell death at baseline, but when treated with tunicamycin, a chemotherapeutic which blocks N-linked glycosylation and induces death via the unfolded protein response, significant heterogeneity in cell death sensitivity was observed between all clonal lines. Viability varied between 12–77% for non-edited parental, 17–88% for scrambled, and 8–52% for *NLRP1*-edited MOLT-4 clones (Fig. 1d).

The sensitivity or resistance of clonal cell lines to chemotherapeutics was maintained across multiple experiments (Fig. 2a, b). Overall, these data indicate considerable phenotypic

heterogeneity between single-cell clones from the Jurkat and MOLT-4 human T-cell line following exposure to cytotoxic chemotherapeutic agents.

Shared and unique mutations in single-cell clones

We hypothesized that genetic aberrations might underlie the wide variation in cell death responses to cytotoxic chemotherapeutics between clones. To investigate the contribution of genetic changes to cell death stimuli, we conducted whole genome sequencing at a depth of 30x on two MOLT-4 *NLRP1*-edited clones, and the original MOLT-4 parental cell line that had not undergone electroporation and was not derived from a single cell cloning process. Structural variants, which include duplications, deletions, inversions, and translocations unique to the clonal *NLRP1*-edited cell lines were analyzed. We identified several shared and unique translocation events among the *NLRP1*-edited clonal lines, along with 29 structural variants shared between clone 1 and clone 2, 17 structural variants unique to clone 1, and 16 structural variants unique to clone 2 (Fig. 3a, b). To determine if the structural variants were predicted sites of off-target CRISPR/Cas9 editing, we used Cas-OFFinder [14] to search the genome for potential off-target sites in a user-defined sequence. No evidence of off-target editing was identified that could explain the structural variants seen in the whole genome sequencing data of the two *NLRP1*-edited clones. These data suggest that unique variants may reflect the genetic instability of MOLT-4 T-cells, whereas shared variants either reflect common ancestry in the MOLT-4 population or off-target sites not predicted by current prediction algorithms for CRISPR-Cas9 editing.

A number of structural variants unique to the clonal lines were identified in genes responsible for both cell survival and metabolism of chemotherapeutic agents, which could help explain the variability in cell death response between clones (Table 1). Variants shared between the two *NLRP1*-edited clones included: *CDK6*, which promotes the G1/S cell cycle transition [17]; *MYB*, which acts as a tumor suppressor [18]; *MIR137*, which is implicated as a tumor suppressor [19]; *FGF12*, which modulates voltage gated sodium channels and has an anti-apoptotic effect [20]; and *RANGAP1*, which is involved in glucuronidation and drug resistance [21]. Additional unique structural variants identified in Clone 1 were located at the locus for: *HINT1*, which acts as a tumor suppressor [22]; *POLE2*, which is an accessory subunit of DNA polymerase epsilon 2 with anti-tumor activity [23]; and *UGT2B17*, which is involved in glucuronidation [24]. Clone 2 had unique variants in: *TERB2*, which is involved in meiotic telomere attachment to the nucleus inner membrane [13]; and *CYP2A6*, which is a member of the cytochrome P450 superfamily and can catalyze the metabolism of anti-cancer drugs [25]. The genetic heterogeneity of human T-cell populations and corresponding stable cell death phenotypes of single-cell clones may serve as a useful screening tool to identify novel genetic variants that could contribute to differential responses to chemotherapeutics in cell types more tractable to CRISPR-Cas9 genome editing and experimental validation.

We hypothesized that the numerous unique and shared mutations between the two clonal lines may represent the genetic heterogeneity present in the parental population, the genetic instability of human leukemic cell lines, and/or off target CRISPR-Cas9 effects not predicted by current algorithms. To address this, we recalled 12 of the structural variants found in the

clones, including variants unique to and shared between clone 1 and clone 2, in the parental line and visualized read support. The majority of variants present in the two clones were not identified in reads from WGS of the parental line. Some variants, including MYB and TPM3P9 – were present at low abundance in the parental line with 1 or 2 reads.

DISCUSSION

In this study we characterize the cell death response of clonal human T-cell lines to chemotherapeutics following CRISPR-Cas9 genetic editing and single-cell cloning. Single cell clones were derived from the parental T-cell population in two ways: (1) following single cell cloning without electroporation; or (2) following electroporation with a scrambled sgRNA RNP or *NLRP1*-targeted sgRNA RNP. All clonal populations demonstrated a wide range in sensitivity to chemotherapeutics, but maintained a stable profile of responses across multiple experiments.

The enduring phenotypic differences observed in this study may be attributed to mutations that arose early in the cloning process or were already sub-clones in the parental population before cloning commenced. Interestingly, the cloning process did not select only for cells that were more resistant to death. Instead, many clonal cell lines were more sensitive to death than the parental non-clonal cell line, despite similar viability at baseline. Numerous variants identified in pathways related to cell death and metabolism likely explain the phenotypic spectrum of the single-cell clones. A few structural variants found in the clones showed a small amount of read support in the parental line, however the majority of genetic variants in the clonal lines were not found in any reads from the parental line. We conclude that while some of the structural variants may have been sub-clones present in the parental population at a very low percentage, the majority of variants represent novel mutations introduced during the cloning process due to genetic instability of human T-cell lines, or alternatively, off-target CRISPR-Cas9 effects not predicted by current algorithms. Future studies such as sequencing of parental clones and scrambled clones, as well as single cell sequencing, or deeper sequencing, of the non-clonal parental line could help confirm this hypothesis.

These data demonstrate the variability of cell death responses between single-cell clones isolated from the same population, and highlight these phenomena as a factor that must be considered in assay design when death of cells can influence genome-wide screens as well as in analysis of single-cell clones to study gene function. In addition to generating an equivalent number of negative controls as test clones to estimate the variation in phenotype between clones, we suggest that rescue assays be considered to conclude a phenotype is due to a specific targeted perturbation. In addition, effects should be evident in short-term bulk assays in which the possibility to be misled by clonal variation is substantially reduced. In terms of screens, appropriate screen design can help mitigate this concern by ensuring adequate representation in terms of cells per individual perturbation, appropriate positive and negative controls and biological replicates, and appropriate statistical analysis. In addition, validation of findings is critical not only in single-cell clones but in bulk populations. This is particularly important where cellular stresses such as chemotherapeutics are used to interrogate biochemical pathways. Overall, our study demonstrates the

importance of considering cellular heterogeneity when designing experiments that act at the level of single cells.

Acknowledgments

Funding: This work was supported by the V Foundation for Cancer Research, The Alex's Lemonade Stand Foundation, The Gabrielle's Angel Foundation for Cancer Research, the National Institute of Health grant R56 AI103352, and the Howard Hughes Medical Institute Medical Student Research Fellowship. Work by LP and JNH at the Harvard Chan Bioinformatics Core and the Center for Stem Cell Bioinformatics was supported by funding from the Harvard Stem Cell Institute.

References

[1]. Shalem O, Sanjana NE, Hartenian E, Shi X, Scott DA, Mikkelsen TS, et al. Genome-scale crispr-cas9 knockout screening in human cells. Science 2014;343:84 DOI: 10.1126/science.1247005. [PubMed: 24336571]

[2]. Shalem O, Sanjana NE, and Zhang F. High-throughput functional genomics using crispr–cas9. Nat Rev Genet 2015;16:299 DOI: 10.1038/nrg3899. [PubMed: 25854182]

[3]. Cox DBT, Platt RJ, and Zhang F. Therapeutic genome editing: Prospects and challenges. Nat Med 2015;21:121 DOI: 10.1038/nm.3793. [PubMed: 25654603]

[4]. Mandal Pankaj K, Ferreira LMR, Collins R, Meissner Torsten B, Boutwell Christian L, Friesen M, et al. Efficient ablation of genes in human hematopoietic stem and effector cells using crispr/cas9. Cell Stem Cell 2014;15:643–52. DOI: 10.1016/j.stem.2014.10.004. [PubMed: 25517468]

[5]. Jacobi AM, Rettig GR, Turk R, Collingwood MA, Zeiner SA, Quadros RM, et al. Simplified crispr tools for efficient genome editing and streamlined protocols for their delivery into mammalian cells and mouse zygotes. Methods 2017;121–122:16–28. DOI: 10.1016/j.ymeth.2017.03.021.

[6]. Canver MC, Bauer DE, Dass A, Yien YY, Chung J, Masuda T, et al. Characterization of genomic deletion efficiency mediated by clustered regularly interspaced palindromic repeats (crispr)/cas9 nuclease system in mammalian cells. J Biol Chem 2014;289:21312–24. DOI: 10.1074/jbc.M114.564625. [PubMed: 24907273]

[7]. Seki A and Rutz S. Optimized rnp transfection for highly efficient crispr/cas9-mediated gene knockout in primary t cells. J Exp Med 2018;215:985–97. DOI: 10.1084/jem.20171626. [PubMed: 29436394]

[8]. Ran FA, Hsu PD, Wright J, Agarwala V, Scott DA, and Zhang F. Genome engineering using the crispr-cas9 system. Nat Protoc 2013;8:2281 DOI: 10.1038/nprot.2013.143. [PubMed: 24157548]

[9]. McGranahan N and Swanton C. Clonal heterogeneity and tumor evolution: Past, present, and the future. Cell 2017;168:613–28. DOI: 10.1016/j.cell.2017.01.018. [PubMed: 28187284]

[10]. Spencer SL, Gaudet S, Albeck JG, Burke JM, and Sorger PK. Non-genetic origins of cell-to-cell variability in trail-induced apoptosis. Nature 2009;459:428–32. DOI: 10.1038/nature08012. [PubMed: 19363473]

[11]. Morrissy AS, Garzia L, Shih DJ, Zuyderduyn S, Huang X, Skowron P, et al. Divergent clonal selection dominates medulloblastoma at recurrence. Nature 2016;529:351–7. DOI: 10.1038/nature16478. [PubMed: 26760213]

[12]. Eirew P, Steif A, Khattra J, Ha G, Yap D, Farahani H, et al. Dynamics of genomic clones in breast cancer patient xenografts at single-cell resolution. Nature 2015;518:422–6. DOI: 10.1038/nature13952. [PubMed: 25470049]

[13]. Ben-David U, Ha G, Tseng YY, Greenwald NF, Oh C, Shih J, et al. Patient-derived xenografts undergo mouse-specific tumor evolution. Nat Genet 2017;49:1567–75. DOI: 10.1038/ng.3967. [PubMed: 28991255]

[14]. Bae S, Park J, and Kim J-S. Cas-offinder: A fast and versatile algorithm that searches for potential off-target sites of cas9 rna-guided endonucleases. Bioinformatics 2014;30:1473–5. DOI: 10.1093/bioinformatics/btu048. [PubMed: 24463181]

[15]. Fu Y, Foden JA, Khayter C, Maeder ML, Reyon D, Joung JK, et al. High frequency off-target mutagenesis induced by crispr-cas nucleases in human cells. Nat Biotechnol 2013;31:822–6. DOI: 10.1038/nbt.2623. [PubMed: 23792628]

[16]. Sidow A, Spies N, Salit M, and Zook JM. Svviz: A read viewer for validating structural variants. Bioinformatics 2015;31:3994–6. DOI: 10.1093/bioinformatics/btv478. [PubMed: 26286809]

[17]. Tigan AS, Bellutti F, Kollmann K, Tebb G, and Sexl V. Cdk6—a review of the past and a glimpse into the future: From cell-cycle control to transcriptional regulation. Oncogene 2015;35:3083 DOI: 10.1038/onc.2015.407. [PubMed: 26500059]

[18]. Ramsay RG and Gonda TJ. Myb function in normal and cancer cells. Nat Rev Cancer 2008;8:523 DOI: 10.1038/nrc2439. [PubMed: 18574464]

[19]. Nilsson EM, Laursen KB, Whitchurch J, McWilliam A, Odum N, Persson JL, et al. Mir137 is an androgen regulated repressor of an extended network of transcriptional coregulators. Oncotarget 2015;6:35710–25. DOI: 10.18632/oncotarget.5958. [PubMed: 26461474]

[20]. Nakayama F, Yasuda T, Umeda S, Asada M, Imamura T, Meineke V, et al. Fibroblast growth factor-12 (fgf12) translocation into intestinal epithelial cells is dependent on a novel cell-penetrating peptide domain: Involvement of internalization in the in vivo role of exogenous fgf12. J Biol Chem 2011;286:25823–34. DOI: 10.1074/jbc.M110.198267. [PubMed: 21518765]

[21]. Cummings J, Ethell BT, Jardine L, Boyd G, Macpherson JS, Burchell B, et al. Glucuronidation as a mechanism of intrinsic drug resistance in human colon cancer: Reversal of resistance by food additives. Cancer Res 2003;63:8443–50. [PubMed: 14679008]

[22]. Weiske J and Huber O. The histidine triad protein hint1 triggers apoptosis independent of its enzymatic activity. J Biol Chem 2006;281:27356–66. DOI: 10.1074/jbc.M513452200. [PubMed: 16835243]

[23]. Li J, Wang J, Yu J, Zhao Y, Dong Y, Fan Y, et al. Knockdown of pole2 expression suppresses lung adenocarcinoma cell malignant phenotypes in vitro. Oncol Rep 2018;40:2477–86. DOI: 10.3892/or.2018.6659. [PubMed: 30132567]

[24]. Zhang H, Basit A, Busch D, Yabut K, Bhatt DK, Drozdzik M, et al. Quantitative characterization of udp-glucuronosyltransferase 2b17 in human liver and intestine and its role in testosterone first-pass metabolism. Biochem Pharmacol 2018;156:32–42. DOI: 10.1016/j.bcp.2018.08.003. [PubMed: 30086285]

[25]. Komatsu T, Yamazaki H, Shimada N, Nakajima M, and Yokoi T. Roles of cytochromes p450 1a2, 2a6, and 2c8 in 5-fluorouracil formation from tegafur, an anticancer prodrug, in human liver microsomes. Drug Metab Dispos 2000;28:1457–63. [PubMed: 11095583]

[26]. Giakountis A, Moulos P, Sarris ME, Hatzis P, and Talianidis I. Smyd3-associated regulatory pathways in cancer. Semin Cancer Biol 2017;42:70–80. DOI: 10.1016/j.semcancer.2016.08.008. [PubMed: 27554136]

[27]. Nilsson EM, Laursen KB, Whitchurch J, McWilliam A, Ødum N, Persson JL, et al. Mir137 is an androgen regulated repressor of an extended network of transcriptional coregulators. Oncotarget 2015;6:35710–25. DOI: 10.18632/oncotarget.5958. [PubMed: 26461474]

[28]. Wright C, Gupta CN, Chen J, Patel V, Calhoun VD, Ehrlich S, et al. Polymorphisms in mir137hg and microrna-137-regulated genes influence gray matter structure in schizophrenia. Translational Psychiatry 2016;6:e724–e. DOI: 10.1038/tp.2015.211. [PubMed: 26836412]

[29]. Duan J, Shi J, Fiorentino A, Leites C, Chen X, Moy W, et al. A rare functional noncoding variant at the gwas-implicated mir137/mir2682 locus might confer risk to schizophrenia and bipolar disorder. Am J Hum Genet 2014;95:744–53. DOI: 10.1016/j.ajhg.2014.11.001. [PubMed: 25434007]

[30]. Mihara S and Suzuki N. Role of txk, a member of the tec family of tyrosine kinases, in immune-inflammatory diseases. Int Rev Immunol 2007;26:333–48. DOI: 10.1080/08830180701690835. [PubMed: 18027204]

[31]. Stavraka C and Blagden S. The la-related proteins, a family with connections to cancer. Biomolecules 2015;5:2701–22. DOI: 10.3390/biom5042701. [PubMed: 26501340]

[32]. Shi X, Tan H, Le X, Xian H, Li X, Huang K, et al. An expression signature model to predict lung adenocarcinoma-specific survival. Cancer Manag Res 2018;10:3717–32. DOI: 10.2147/CMAR.S159563. [PubMed: 30288103]

[33]. Yoshikawa Y, Satoh T, Tamura T, Wei P, Bilasy SE, Edamatsu H, et al. The m-ras-ra-gef-2-rap1 pathway mediates tumor necrosis factor-alpha dependent regulation of integrin activation in splenocytes. Mol Biol Cell 2007;18:2949–59. DOI: 10.1091/mbc.e07-03-0250. [PubMed: 17538012]

[34]. Hsiao YC, Tong ZJ, Westfall JE, Ault JG, Page-McCaw PS, and Ferland RJ. Ahi1, whose human ortholog is mutated in joubert syndrome, is required for rab8a localization, ciliogenesis and vesicle trafficking. Hum Mol Genet 2009;18:3926–41. DOI: 10.1093/hmg/ddp335. [PubMed: 19625297]

[35]. Lapierre M, Linares A, Dalvai M, Duraffourd C, Bonnet S, Boulahtouf A, et al. Histone deacetylase 9 regulates breast cancer cell proliferation and the response to histone deacetylase inhibitors. Oncotarget 2016;7:19693–708. DOI: 10.18632/oncotarget.7564. [PubMed: 26930713]

[36]. Giacomini CP, Sun S, Varma S, Shain AH, Giacomini MM, Balagtas J, et al. Breakpoint analysis of transcriptional and genomic profiles uncovers novel gene fusions spanning multiple human cancer types. PLoS Genet 2013;9:e1003464 DOI: 10.1371/journal.pgen.1003464. [PubMed: 23637631]

[37]. Ikenouchi J and Umeda M. Frmd4a regulates epithelial polarity by connecting arf6 activation with the par complex. Proc Natl Acad Sci U S A 2010;107:748–53. DOI: 10.1073/pnas.0908423107. [PubMed: 20080746]

[38]. Maeda N Inheritance of the human salivary proline-rich proteins: A reinterpretation in terms of six loci forming two subfamilies. Biochem Genet 1985;23:455–64. DOI: 10.1007/BF00499086. [PubMed: 3840016]

[39]. Clark AA, Dotson CD, Elson AE, Voigt A, Boehm U, Meyerhof W, et al. Tas2r bitter taste receptors regulate thyroid function. FASEB J 2015;29:164–72. DOI: 10.1096/fj.14-262246. [PubMed: 25342133]

[40]. Chin K-T, Xu H-T, Ching Y-P, and Jin D-Y. Differential subcellular localization and activity of kelch repeat proteins klhdc1 and klhdc2. Mol Cell Biochem 2007;296:109–19. DOI: 10.1007/s11010-006-9304-6. [PubMed: 16964437]

[41]. Shao S, Brown A, Santhanam B, and Hegde Ramanujan S. Structure and assemblypathway of the ribosome quality control complex. Mol Cell 2015;57:433–44. DOI: 10.1016/j.molcel.2014.12.015. [PubMed: 25578875]

[42]. Shibuya H, Hernández-Hernández A, Morimoto A, Negishi L, Höög C, and Watanabe Y. Majin links telomeric DNA to the nuclear membrane by exchanging telomere cap. Cell 2015;163:1252–66. DOI: 10.1016/j.cell.2015.10.030. [PubMed: 26548954]

[43]. Iwata T, Popescu NC, Zimonjic DB, Karlsson C, Hoog JO, Vaca G, et al. Structural organization of the human sorbitol dehydrogenase gene (sord). Genomics 1995;26:55–62. DOI: 10.1016/0888-7543(95)80082-W. [PubMed: 7782086]

[44]. Sørensen JB. Ride the wave: Retrograde trafficking becomes ca(2+) dependent with baiap3. J Cell Biol 2017;216:1887–9. DOI: 10.1083/jcb.201706007. [PubMed: 28626002]

[45]. Liu J, Ji X, Li Z, Yang X, Wang W, and Zhang X. G protein γ subunit 7 induces autophagy and inhibits cell division. Oncotarget 2016;7:24832–47. DOI: 10.18632/oncotarget.8559. [PubMed: 27056891]

[46]. Zeng J-H, Liang L, He R-Q, Tang R-X, Cai X-Y, Chen J-Q, et al. Comprehensive investigation of a novel differentially expressed lncrna expression profile signature to assess the survival of patients with colorectal adenocarcinoma. Oncotarget 2017;8:16811–28. DOI: 10.18632/oncotarget.15161. [PubMed: 28187432]

[47]. Dietrich J, Cella M, Seiffert M, Bühring H-J, and Colonna M. Cutting edge: Signal-regulatory protein β1 is a dap12-associated activating receptor expressed in myeloid cells. J Immunol 2000;164:9 DOI: 10.4049/jimmunol.164.1.9. [PubMed: 10604985]

Highlights

1. Genetic heterogeneity in human T-ALL cell lines contributes to large differences in cell death responses, and could explain failure of induction therapy.
2. Single cell T-ALL clones do not revert to parental phenotype, or resemble the parental phenotype of a population of genetically-diverse T-ALL cells

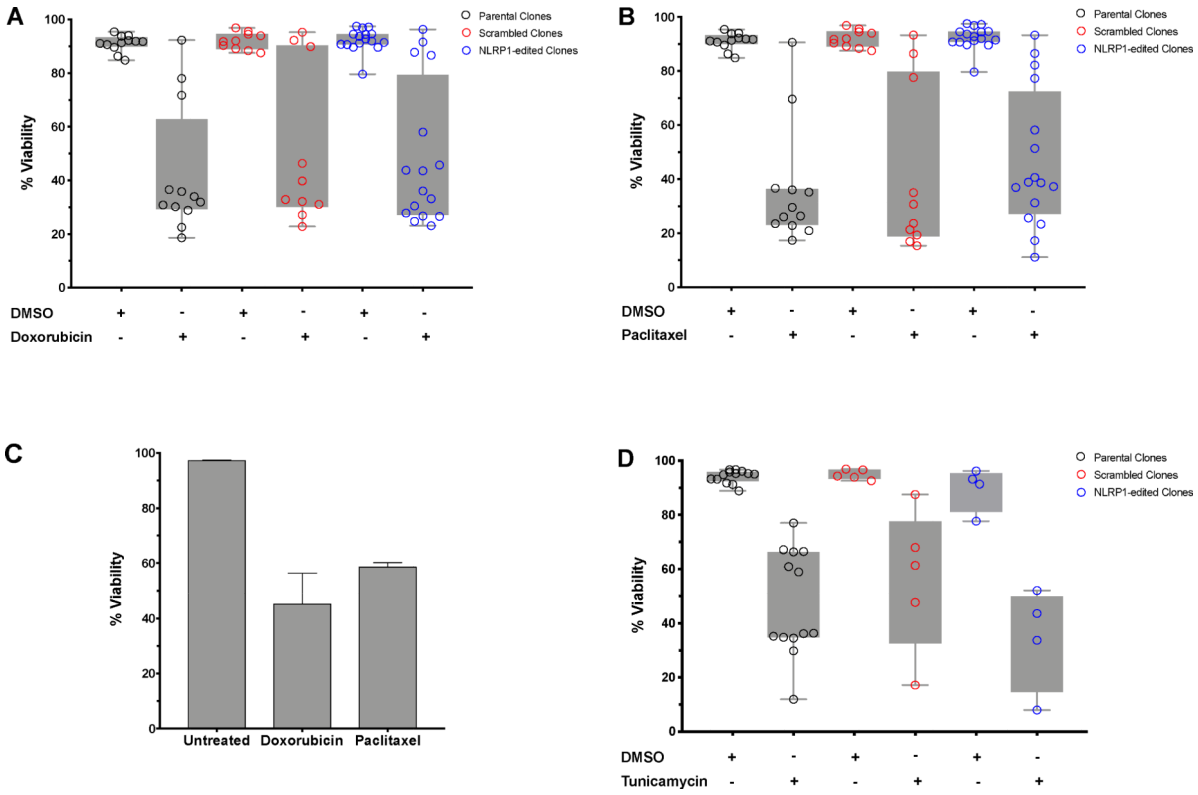

Figure 1. Wide range in viability of Jurkat and MOLT-4 clonal cell lines after treatment with chemotherapeutics.

Representative plots showing percent viability of non-edited parental, scrambled, or *NLRP1*-edited Jurkat clones after treatment for 48 hours with either 0.1% DMSO or A) 200nM doxorubicin or B) 500nM paclitaxel. C) Percent viability of the non-clonal parental Jurkat cell line after 48 hours of treatment with either 0.1% DMSO, 200nM doxorubicin or 500nM paclitaxel. D) Representative plot showing percent viability of the non-edited parental, scrambled, or *NLRP1*-edited MOLT-4 clones after treatment with either 0.1% DMSO or 1ug/mL tunicamycin for 48 hours. Each dot or bar represents the average of duplicate samples. Cell death was assessed using propidium iodide (PI) staining and flow cytometry, with viable cells classified as PI negative.

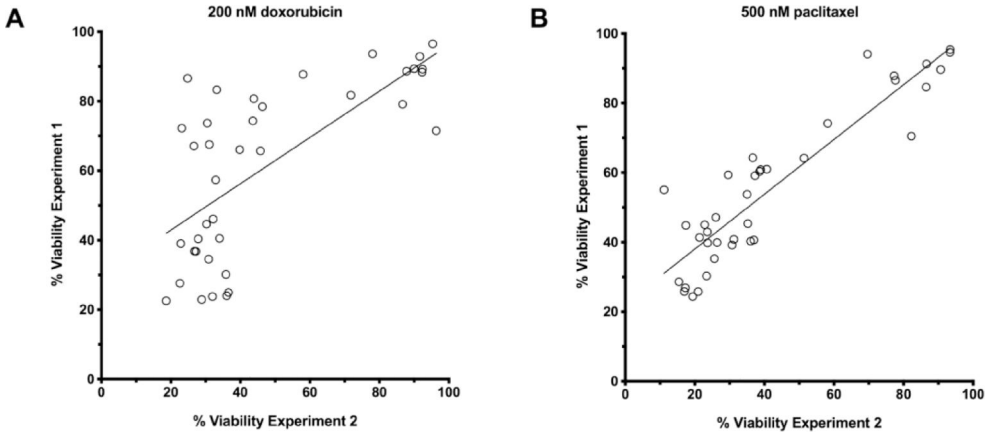

Figure 2. Clonal cell lines maintained their phenotypic response across experiments.

Linear regression lines displaying the viability of the non-edited parental, scrambled, or *NLRP1*-edited clonal cell lines in two experiments after treatment for 48 hours with A) 200nM doxorubicin or B) 500nM paclitaxel. Each circle represents a single clone across two experiments. The y-axis represents the viability of the clone in experiment 1 and the x-axis represents the viability of the clone in experiment 2. The % viability of each clone represents the average of duplicate samples for each experiment. Cell death was assessed using propidium iodide (PI) staining and flow cytometry, with viable cells classified as PI negative.

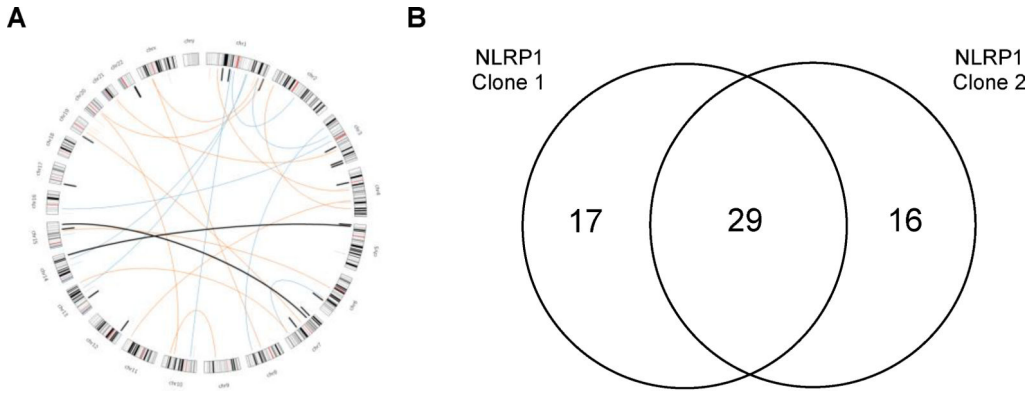

Figure 3. Shared and unique variants and translocations in single-cell clones.

A) Circos plot depicting the common (thick black strikes) and unique (thin strikes) structural variants in *NLRP1*-edited clone 1 (thin blue strike) and clone 2 (thin orange strike) as compared to the MOLT-4 parental cell line. The lines in the interior circle represent chromosomal translocations. B) Venn diagram depicting the number of unique and shared structural variants (inversions, duplications, and deletions) between *NLRP1*-edited clone 1 and clone 2 as compared to the non-edited parental cell line.

Table 1.

Genetic variants unique to two single-cell clones include multiple genes involved in drug metabolism, cell division, and cell death.

Size (base pairs), position, type of mutation, and function of the genetic variants unique to either or both *NLRP1*-edited clone 1 and clone 2 as compared to the parental cell line. Chr., Chromosome; NA, Not Applicable (the mutation is not found in the clone); –, no primary literature was found on the gene of interest by the authors, ensemble was then searched to confirm the gene function is unknown.

Gene	Mutation	Chr.	Position Clone 1	Position Clone 2	Size Clone 1	Size Clone 2	Gene Function
HNRNPCL	Duplication	1	NA	209111023	NA	54775	–
HNRNPCL3	Duplication	1	NA	12894968	NA	54786	–
PRAMEF2	Duplication	1	NA	12894968	NA	54786	–
PRAMEF4	Duplication	1	NA	12894968	NA	54786	–
HNRNPCL1	Duplication	1	NA	12894968	NA	54786	–
SMYD3	Deletion	1	246065672	246065672	69676	69676	Methyltransferase; oncogene[26]
MIR137	Duplication	1	98428838	98428838	121893	121893	Implicated in tumor suppression[27]
MIR137HG	Duplication	1	98428838	98428838	121893	121893	Implicated in schizophrenia[28]
MIR2682	Duplication	1	98428838	98428838	121893	121893	Implicated in schizophrenia[29]
RP5–1051D14.1	Duplication	1	NA	209111023	NA	54775	–
RPS7P4	Deletion	1	68712878	68712878	51	51	Pseudogene
PTMAP8	Deletion	3	116742232	116742232	102963	102963	Pseudogene
RP11–416O18.2	Duplication	3	181799895	181799872	110163	110186	–
FGF12	Duplication	3	191834767	191834767	62222	62222	Pro-survival[20]
C4orf29	Duplication	4	128962761	NA	17910	NA	–
RP11–149A7.2& RP11–404I7.2	Inversion	4	NA	133560780	NA	304899	–
UGT2B17	Duplication	4	69374436	NA	117321	NA	Glucuronidation[24]
TXK	Inversion	4	48111843	48111843	137	137	Th1-cell development & IFNγ regulation[30]
LARP1B	Duplication	4	128962761	NA	17910	NA	Function unknown[31]
RP11–445O3.1	Duplication	5	4474094	4474094	102974	102974	LncRNA, function unknown[32]
HINT1	Duplication	5	130473349	NA	27629	NA	Tumor suppressor[22]
RAPGEF6	Deletion	5	130804190	NA	87	NA	Guanine exchange factor[33]
AHI1	Duplication	6	135474112	135474112	328110	328110	Vesicle trafficking[34]
MYB	Duplication	6	135474112	135474112	328110	328110	Proto-oncogene[18]
CDK6	Inversion	7	92197467	92197467	87795	87795	Cell cycle regulation[17]
HDAC9	Duplication	7	18827254	18827254	44648	44648	Histone deacetylase; proliferation[35]
FAM133B	Inversion	7	92197313	92197467	27948	87795	Fusion with CDK6 found in ALL[36]
FRMD4AX	Deletion	10	14377265	NA	572	NA	Regulation of epithelial cell polarity[37]

Gene	Mutation	Chr.	Position Clone 1	Position Clone 2	Size Clone 1	Size Clone 2	Gene Function
PRB4	Duplication	12	11295165	11295165	51849	51849	Glycoprotein involved in taste[38]
SMIM10L1	Duplication	12	11295165	11295165	51849	51849	–
PRH1-PRR4	Duplication	12	11295165	11295165	51849	51849	–
TAS2R42	Duplication	12	11295165	11295165	51849	51849	Taste receptor; thyroid function[39]
ELF1	Duplication	13	41481543	41481543	53481	53481	Hematopoiesis transcription factor
RN7SL761P	Duplication	13	69153798	NA	133490	NA	Pseudogene
RPL12P34	Duplication	13	69153798	NA	133490	NA	–
RPS3AP52	Duplication	13	69153798	NA	133490	NA	Pseudogene
SUGT1P3	Duplication	13	41481543	41481543	53481	53481	Pseudogene
TPTE2P5	Duplication	13	41481543	41481543	53481	53481	Pseudogene
KLHDC1	Duplication	14	50124869	NA	154659	NA	–
KLHDC2	Duplication	14	50124869	NA	154659	NA	Muscle cell migration and differentiation[40]
NEMF	Duplication	14	50124869	NA	154659	NA	Ubiquitination[41]
POLE2	Duplication	14	50124869	NA	154659	NA	DNA polymerase epsilon[23]
RP11–279F6.3	Duplication	15	69869159	69869159	81066	81066	Tumor suppressor in prostate cancer[6]
TERB2	Inversion	15	45131353	NA	222296	NA	Telomere functione[42]
SORD	Inversion	15	45131353	NA	222296	NA	Sorbitol dehydrogenase[43]
BAIAP3	Duplication	16	NA	1389751	NA	653	Golgi trafficking[44]
NLRP1	Deletion	17	5461610	5461610	1855	1855	CRISPR/Cas9 Targeted Protein
AC006273.4	Deletion	19	776189	776185	1479	1494	–
ACC006273.4	Duplication	19	777706	NA	404	NA	–
CYP2A6	Duplication	19	NA	41346432	NA	30611	Drug metabolism[25]
ZNF761	Deletion	19	NA	53899801	NA	73521	–
ZNF765	Deletion	19	NA	53899801	NA	73521	–
ZNF813	Deletion	19	NA	53899801	NA	73521	–
TPM3P9	Deletion	19	NA	53899801	NA	73521	Pseudogene
GNG7	Deletion	19	2603957	NA	14633	NA	Autophagy and cell division[45]
AC006273.5	Duplication	19	777706	NA	404	NA	LncRNA[46]
CTB-50L17.2	Inversion	19	NA	4611961	NA	5070	Pseudogene
SIRPB1	Deletion	20	NA	1557463	NA	33027	Tyrosine phosphorylation[47]
CHODL	Duplication	21	NA	19522067	NA	99874	–
ZC3H7B	Duplication	22	41666977	41666977	80050	80050	Zinc finger protein
MPPED1	Duplication	22	43793951	43793951	88042	88042	–
RANGAP1	Duplication	22	41666977	41666977	80050	80050	Glucuronidation & drug resistance[21]
HTR2C	Duplication	X	NA	114146533	NA	26370	Serotonin Receptor[35]